International Journal of Research in Engineering and Innovation (IJREI)
journal home page: http://www.ijrei.com
ISSN (Online): 2456-6934

Numerical investigation of fluid flow and aerodynamic performance on a 2D NACA-4412 airfoil

Husain Mehdi, Shwetanshu Gaurav, Mudit Sharma

Department of Mechanical Engineering, Meerut Institute of Technology, Meerut, India

Abstract

The performance of an aircraft wing mostly depend on the aerodynamic characteristics i.e. lift force, drag force, pressure distribution, ratio of lift to drag etc. In this paper the influence of aerodynamic performance on two dimensional NACA 4412 airfoil is investigated. The computational method consist of steady state, incompressible, finite volume method, spalart-allmaras turbulence model. The flow has been studied with the help of Navier-Stroke and continuity equations. Numerical simulations were performing at Reynolds number ($1x10^6$, $2x10^6$, $3x10^6$, and $4x10^6$) at different angle of attack (0^0, 3^0,6^0, and 9^0). The results give the satisfactory measure of confidence of fidelity of the simulation. Aerodynamic forces are calculated with different Reynolds number and angle of attack, after analyzing the data it is found that the higher lift coefficient was obtain in Re-$4x10^6$ at angle of attack 9^0 whereas low drag coefficient was obtain in Re-$1x10^6$ at AOA-0^0

© 2016 ijrei.com. All rights reserved

Key words: Reynolds Number, Lift coefficient Drag coefficient NACA 4412, Angle of attack

1. Introduction

In recent years, several studies have been published using viscous numerical methods to solve two-dimensional incompressible flows around airfoils in ground effect. A finite volume method employing the k-ε turbulence model was used on an NACA 4412 airfoil [1].

A simple approach for experiment on aerodynamic static stability analysis of different types of wing shapes. They tested the reduced scale size wings of different shapes like rectangular, rectangular with curved tip, tapered, tapered with curved tip, etc. in low speed subsonic wind tunnel at different air speeds and different angles of attack. The authors found that the tapered wing with curved tip was the most stable at different speeds and ranges of working angles of attack [2]. Various types of Wing-in-Ground (WIG) craft, mainly experimental, were constructed and tested in the last century. High-speed, high-payload marine and amphibious transportation means benefit from using aerodynamic lift enhanced in ground vicinity [3]. A circular planform non-spinning body with an airfoil section configuration developed and produced by Geobat Flying Saucer Aviation Inc. in the Auburn University wind tunnel facility. For comparison purpose, a Cessna 172 model was also tested. The author found that the lift curve slope of the Geobat was less than that of Cessna 172 but displayed better stall characteristics [4]

The two-dimensional characteristics of airfoil NACA 0018 are modeled for the medium range Reynolds numbers between 300,000 and 1000,000 and angle of attack (a) between 0 and 25 to establish the lift and drag coefficients. Between all the investigated models, the k–ω SST model gives the most accurate predictions for C_L and C_D compared with the available experimental data for all the investigated range of Re numbers [5].

It has been studied and presented basic results from wing planform optimization for minimum drag with constraints on structural weight and maximum lift [6]. The aerodynamic characteristics analysis for different airfoils have also been conducted at different corners of the world [7]. Airfoil is one of the basic parts of the wind turbine blade designs. Aerodynamic characteristics of rotor significantly depend on the airfoil-shaped blades. Purpose and efficiency of airfoil is to create a low pressure area over the blades to generate lift force, also the drag force is produced unintentionally [8]. The effectiveness of an airfoil with bi-camber surface]

studied the fluid flow and aerodynamic forces on an airfoil

Corresponding author: Husain Mehdi
Email Address: husainmehdi4u@gmail.com

[9]. The impact of Atmosphere Boundary Layer (ABL) is low in the height at which wind turbines are usually installed and the wind is almost calm. Atmosphere Boundary Layer (ABL) depends on the topology and the surface roughness. If turbines work in urban areas or areas with rough surface, wind speed is reduced under the atmospheric boundary layer influence [10].

Fluid Structure Interaction of uniform flow past a two dimensional pleated airfoil is carried out. When the wing interact with the air, it is subjected to both aerodynamic forces acting on the surface of the wing and the inertial force due to the acceleration of deceleration of the wing mass. The interaction between these inertial and aerodynamic forces resulted in wing deformation. In the first phase of the work, fluid flow simulation at Reynolds Number-100, 200, 500, and 1000 will be performed with angle of attack 0^0 to 15^0, it was found that for all the simulations performed flow always remained steady at Re 100 and 200. First unsteady flow was obtained at Re 500 and AOA 10^0. But flow always remained steady at AOA 0^0 and 5^0 for all the Reynolds numbers [11] [12] [13] [14].

The variation of pressure distribution over an airfoil with Reynold's Number. The flow behavior around an airfoil body has been studied [15], [16].

2. Governing Equation

2.1 Fluid Flow

The solver employs a time-dependent, conservative form of the incompressible Navier-Stokes equations discretized with a finite-volume approach. The incompressible Navier-Stokes equations written in tensor form are

$$\frac{\partial \mathrm{U_i}}{\partial \mathrm{x_i}}=0 \tag{1}$$

$$\frac{\partial \mathrm{U_i}}{\partial \mathrm{t}}+\frac{\partial(\mathrm{U_iU_j})}{\partial \mathrm{x_j}}=-\frac{1}{\rho}\frac{\partial \mathrm{P}}{\partial \mathrm{x_i}}+\upsilon\frac{\partial}{\partial \mathrm{x_j}}\left(\frac{\partial \mathrm{U_i}}{\partial \mathrm{x_j}}\right) \tag{2}$$

Where the indices, i = 1, 2, 3, represent the x, y and z directions, respectively; and the velocity components are denoted by U_1, U_2, and U_3 corresponding to U, V, W respectively. The equations are non-dimensionalized with the appropriate length and velocity scales, The Navier-Stokes equations are discretized using a cell-centered, non-staggered arrangement. In addition to the cell-center velocities, the face-center velocities are computed and used for calculating the volume flux of each cell. The tensor equations in (2) are written as

$$\frac{\partial \mathrm{u_i}}{\partial \mathrm{t}}+\frac{\partial(\mathrm{u_iu_j})}{\partial \mathrm{x_j}}=-\frac{\partial \mathrm{p}}{\partial \mathrm{x_i}}+\frac{1}{\mathrm{Re}}\frac{\partial^2 \mathrm{u_i}}{\partial \mathrm{x_j}\partial \mathrm{x_j}} \tag{3}$$

$$\frac{\partial \mathrm{u_i}}{\partial \mathrm{x_i}}=0 \tag{4}$$

Where Re corresponds to the Reynolds number and is defined as

$$\mathrm{Re}=\frac{\rho \mathrm{U_o c}}{\mu} \tag{5}$$

Here, ρ and μ are density and dynamic viscosity of the fluid.

2.2 Transport Equation for the Spalart-Allmaras Model

The transported variable in the Spalart-Allmaras model $\tilde{\nu}$ is identical to the turbulent kinematic viscosity except in the near-wall (viscosity-affected) region. The transport equation for $\tilde{\nu}$ is

$$\frac{\partial}{\partial \mathrm{t}}(\rho\tilde{\nu})+\frac{\partial}{\partial \mathrm{x_i}}(\rho\tilde{\nu}\mathrm{u_i})=\mathrm{G}\nu+\frac{1}{\sigma_\nu}\left[\frac{\partial}{\partial \mathrm{x_j}}\left\{(\mu+\rho\nu)\frac{\partial \nu}{\partial x_j}\right\}+\mathrm{C_{b20}}\left[\frac{\partial \nu}{\partial \mathrm{x_j}}\right]^2\right]-Y_\nu+S_\nu \tag{6}$$

where G_ν is the production of turbulent viscosity, and Y_ν is the destruction of turbulent viscosity that occurs in the near-wall region due to wall blocking and viscous damping. σ_ν and C_{b2} are the constants and ν is the molecular kinematic viscosity. S_ν is a user-defined source term. Note that since the turbulence kinetic energy k , is not calculated in the Spalart-Allmaras model.

2.3 k-epsilon model

k-epsilon mdel can be derived as

$$\frac{\partial}{\partial t}(\rho k)+\frac{\partial}{\partial x_i}(\rho k u_i)=\frac{\partial}{\partial x_j}\left[\left(\mu+\frac{\mu_t}{\sigma_k}\right)\frac{\partial k}{\partial x_j}\right]+P_k+P_b-\rho\varepsilon-Y_M+S_k \tag{7}$$

$$\frac{\partial}{\partial t}(\rho\varepsilon)+\frac{\partial}{\partial x_i}(\rho\varepsilon u_i)=\frac{\partial}{\partial x_j}\left[\left(\mu+\frac{\mu_t}{\sigma_\varepsilon}\right)\frac{\partial \varepsilon}{\partial x_j}\right]+\frac{C_{1\varepsilon}\varepsilon}{k}(P_k+C_{3\varepsilon}P_b)-\frac{C_{2\varepsilon}\rho\varepsilon^2}{k}+S_\varepsilon \tag{8}$$

The turbulent viscosity is modeled as,

$$\mu_t=\frac{\rho C_\mu k^2}{\varepsilon} \tag{9}$$

Production of k can be written as,

$$P_k=\rho\overline{u_i'u_j'}\frac{\partial u_j}{\partial x_i} \tag{10}$$

$$P_k=\mu_t S^2 \tag{11}$$

Where S is the modulus of the mean rate-of-strain tensor, defined as:

$$S\equiv\sqrt{2S_{ij}S_{ij}}$$

The model constants used for these equations are,

$$C_{1\varepsilon}=1.44,\quad C_{2\varepsilon}=1.92,\quad C_{3\varepsilon}=-0.33,\quad C_\mu 0.09,$$
$$\sigma_k=1.0,\quad \sigma_\varepsilon=1.3$$

3 Boundary Condition

The grid divided into two region as shown in figure. A constant velocity u=25 m/sec is imposed on the left side of the grid and the right side set as on outflow region, where the gradient values are set to be zero. The component are taken in accordance with angle of attack. Pressure on the both sides was taken as atmospheric.

(a)

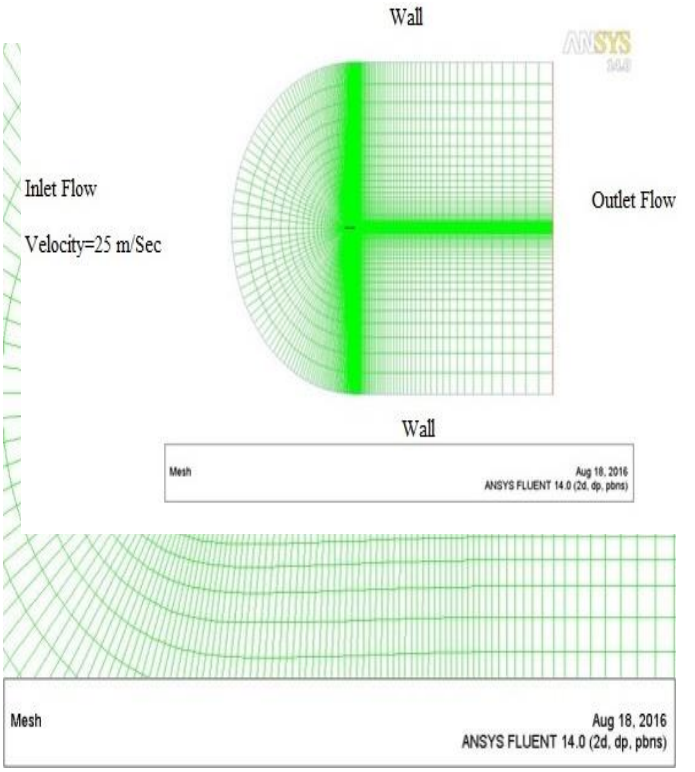

(b)

Figure 1:- (a) Meshing of the airfoil, (b) Zoom view of the meshing

4 Result and Discussion

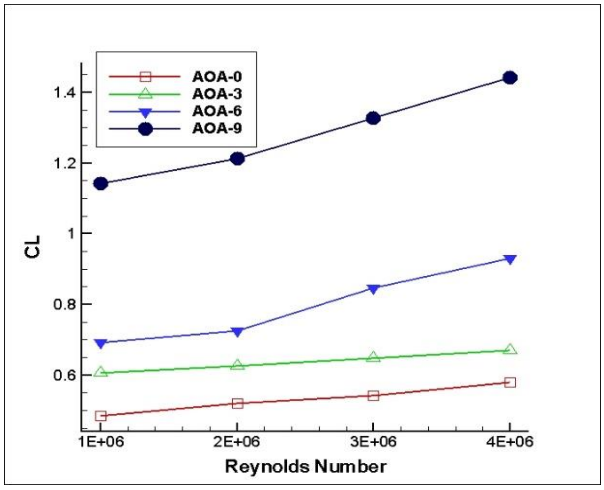

(a)

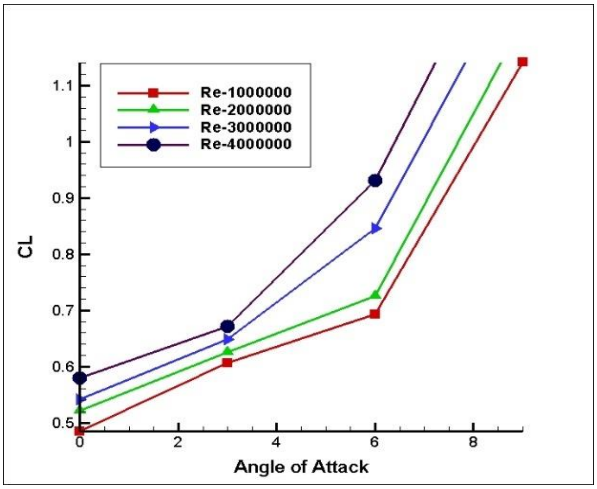

(b)

Figure 2:- Variation of lift coefficient with (a) Reynolds Number, (b) Angle of attack

The curvature is incorporated at the leading edge in such a way that the surface area from the middle of the wing towards the root increase and towards the tip the area decreases in the same rate. The wing can produce more lift due to increased surface area near the root [17].

Variation of lift coefficient with angle of attack and Reynolds number as shown in figure, the greater value of lift coefficient are observed at 9^0 angle of attack at Reynolds number $4x10^6$, whereas minimum value of lift coefficient is observed at 0^0 angle of attack at Reynolds number 10^6

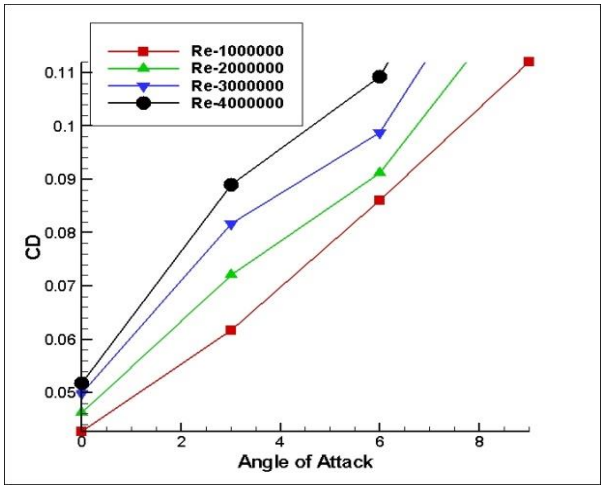

(a)

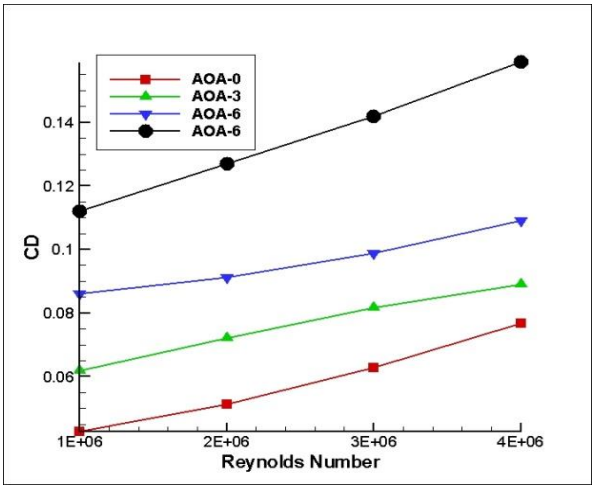

(b)

Figure 3:- Variation of drag coefficient with (a) Reynolds Number, (b) Angle of attack

The pressure below the airfoil to slightly increase as the Reynolds number increases, similarly the suction pressure above the airfoil are also slightly increased, whereas the drag coefficient significantly increases as the flap is deflected. The increase is due to large pressure underneath the airfoil yielding increased pressure drag, along with the growing separation zone on the upper surface of the flap [18].

The mean force coefficients leads to some interesting observations. As expected, the overall drag coefficient increases with increase in Reynolds number, because the viscous effects are more dominant at higher Reynolds numbers which cause the skin friction to be the major contributor to the overall drag. As the angle of attack increased, drag coefficient further increases.

5 Conclusion

In this work CFD simulation are employed to study the flow field and the aerodynamic properties of NACA 4412 airfoil, numerical simulation were performed at Reynolds number ($1x10^6$, $2x10^6$, $3x10^6$, and $4x10^6$) at different angle of attack (0^0, 3^0, 6^0, and 9^0). The result give the satisfactory measure of confidence in the fidelity of the simulation. It was found that the coefficient of drag is increases as the Reynolds number increases. This increase is due to large underneath the airfoil yielding increased pressure drag along with the growing separation zone on the upper surface of the airfoil. The lowest drag coefficient was obtained at Re-$1x10^6$ at angle of attack 0^0, whereas largest lift coefficient was obtained at Re-$4x10^6$ at angle of attack

References

[1] Hsiun and Chen, C. Hsiun, C. Chen, Aerodynamic characteristics of a two-dimensional airfoil with ground effect, Journal of Aircraft, 33 (2) (1996), pp. 33–392.

[2] Dwivedi, Y.D., Prasad, M.S., and Dwivedi, S., "Experimental Aerodynamic Static Stability Analysis of Different Wing Planforms", International Journal of Advancements in Research & Technology, Vol. 2, No. 6,June 2013, pp.60-63.

[3] Rozhdestvensky, K.V. RozhdestvenskyWing-in-Ground effect vehiclesProgress in Aerospace Sciences, 42 (2006), pp. 211–283.

[4] Recktenwald.B , Aerodynamics of a Circular Planform Aircraft", American Institute of Aeronautics andAstronautics 022308, 2008, pp.1-7

[5] Gasser E. Hassan, Amany Hassan, M. Elsayed Youssef., Numerical Investigation of Medium Range Re Number Aerodynamics Characteristics for NACA0018 Airfoil, CFD letters Vol. 6 (4) –December 2014.

[6] Wakayama, S., "Subsonic Wing Planform Design Using Multidisciplinary Optimization", Journal of Aircraft, Vol. 32, No. 4, July-August 1995, pp. 746-753.

[7] Mahmud, M.S., "Analysis of Effectiveness of an Airfoil with Bi-camber Surface", International Journal of Engineering and Technology, Vol. 3, No. 5, May 2013, pp.569-577.

[8] Singh. R. K., Rafiuddin Ahmed, M., Asid Zulla,. M., & Lee. Y. H., Design of A Low Reynolds Number Airfoil For Small Horizontal Axis Wind Turbines. Elsevier, Renewable Energy, 42, 66-76.

[9] Kandwal, S., and Singh, S., "Computational Fluid Dynamics Study of Fluid Flow and Aerodynamic Forces on an Airfoil", International Journal of Engineering and Technology, Vol. 1, No. 7, September 2012, pp.1-8

[10] [Yao, J. Y., Weibin, W., Jianliang, Xie. J., Zhou. H., Peng. M., Sun, Y., (2012). Numerical Simulation of Aerodynamic Performance For Two Dimensional Wind Turbine Airfoils. Elsevier, Energy Procedia, 31, 88-86.

[11] Husain Mehdi, Fahad Anwer, Akhlaque Ahmad,"Fluid Structure Interaction of Flow around a Pleated Insect 2D Airfoil at Ultra Low Reynolds Numbers" International Journal of Research in Aeronautical and Mechanical Engineering, vol.3, issue 3, pp 19-37, 2015.

[12] Syed Fahad Anwer, Intesaaf Ashraf, Husain Mehdi, Akhlaq Ahmad " On the Aerodynamic Performance of Dragon fly wing Section in Gliding Mode" Advances in Aerospace Science and Applications, Vol. 3, pp 227-234, 2013.

[13] Husain Mehdi, Brajesh Kumar, Anil Kamboj"Numerical Analysis of Steady and Unsteady Flow for Dragonfly Wing Section in Gliding Mode"

International Journal of Advanced Mechanical Engineering, Vol.4, pp 365-370, 2014.

[14] Husain Mehdi, Fahad Anwer, Akhlaque Ahmad, "Vibration Analysis of Dragonfly wing section in Gliding Mode at Low Reynolds Number" International Journal of Research in Aeronautical and Mechanical Engineering, vol. 2, issue 12, pp 11-23, 2014.

[15] M.P., "The Variation with Reynolds Number of Pressure Distribution over an Airfoil Section", NACA Report No. 613, pp.65-84 .

[16] Sharma, A., "Evaluation of Flow Behavior around an Airfoil Body", M. Engg thesis, Department of Mechanical Engineering, Thapar University, Patiala-147004, India, July 2012, pp.1-60

[17] M. Nazmul Haque, Mohammad Ali, Ismat Ara, Experimental investigation on the performance of NACA 4412aerofoil with curved leading edge planform,Procedia Engineering 105 (2015) 232 – 240.

[18] Alex E. Ockfen, Konstantin I. Matveev,Aerodynamic characteristics of NACA 4412 airfoil section with flap in extreme ground effect, International Journal of Naval Architecture and Ocean Engineering, Volume 1, Issue 1, (2009), 1–12.

[19] Husain Mehdi, Vipul Namdev, Prashant Kumar, Ashish Tyagi, "Numerical Analysis of Fluid Flow around a Circular Cylinder at Low Reynolds Number", IOSR, Journal of Mechanical and Civil Engineering, vol 3, issue 3, 2016, 94-101.